Steel and Composite Structures, Vol. 10, No. 5 (2010) 373-383
DOI: http://dx.doi.org/10.12989/scs.2010.10.5.373

Experimental studies on composite beams with high-strength steel and concrete

Huiling Zhao*[1] and Yong Yuan[2]

[1]*School of Civil Engineering, Tianjin University, China*
[2]*Department of Geotechnical Engineering, Tongji University, China*

(Received June 17, 2009, Accepted May 26, 2010)

Abstract. This paper presents the experimental studies of the flexural behavior of steel-concrete composite beams. Herein, steel-concrete composite beams were constructed with a welded steel I section beam and concrete slab with different material strength. Four simply supported composite beams subjected to two-point concentrated loads were tested and compared to investigate the effect of high strength engineering materials on the overall flexural response, including failure modes, load deflection behavior, strain response and interface slip. The experimental results show that the moment capacity of composite beams has been improved effectively when high-strength steel and concrete are used. Comparisons of the ultimate flexural strength of beams tested are then made with the calculated results according to the methods specified in guideline Eurocode 4. The ultimate flexural strength based on current codes may be slightly unconservative for predicating the moment capacity of composite beams with high-strength steel or concrete.

Keyword: composite beam; high-strength concrete, flexural behavior.

1. Introduction

Steel-concrete composite beams, consisting of reinforced concrete slabs and steel girders, are widely used in engineering applications. One can take advantages of the benefits of the two construction materials. Reinforced concrete is inexpensive, massive, and stiff, while steel members are strong, lightweight, and easy to assemble Yuna *et al*.(2008). The development of experimental Amadio *et al*.(2004), Lam *et al*.(2005), Nie *et al*.(2004, 2008), Tagawa *et al*.(1989), Uy *et al*.(1998) and analytical research El-Tawil and Deierlein(2001), Liew *et al*.(2001), Richard Liew(2001), Salari and Spacone (2001), Spacone and EI-Tawil(2004), and specifications addressing composite construction, *i.e*., Eurocode 4 Johnson and Anderson(1993), LRFD American Institute of Steel Construction(1994), AIJ-SRC Code Architectural Institute of Japan(1987) and Chinese local codes China Academy of Building Research (2003), are increasingly providing engineers with guidance on the analysis and design of composite beams.

In buildings with wide column spacing and heavy loads, composite beams are often designed as large-dimension cross section. In this case, high strength engineering materials exhibit favorable performance. Composite beams with high strength steel and concrete are required to reduce the height

* Corresponding author, Ms., E-mail: zhaohuiling1668@gmail.com

of floor systems and to achieve a more economical design Yuan *et al*.(2008). Although few design guidelines for composite system with high strength steel and concrete are included in the relative standards and specifications American Institute of Steel Construction(1994), Architectural Institute of Japan(1987), China Academy of Building Research(2003), Johnson and Anderson(1993). In China, the popular structural steel is Q235-steel and Q345-steel. Q235-steel has a nominal yield stress of 235 MPa specified by the manufacturer and Q345-steel has the similar definition. Steel with the yield stress higher than 345 MPa is usually specified as high strength steel and absent in Chinese codes. Recently, high-strength steel and high-strength concrete have become more available. However, their applications in composite beams are limited due to and lack of research and code specifications. High-strength steel and concrete has favorable strength, improved durability and higher resistance to abrasion, but it tends to be more fragile with unnoticeable yield stage and sharp decline after the peak strength. Therefore, the influence of high-strength material on composite beams strength and stiffness may be more pronounced, requiring further exploration.

Some experiments on composite beams with high strength concrete have been conducted in previous research Bullo and Di Marco(2004), Nie *et al*.(2004), Xue and Yang(2009). Studies Nie *et al*.(2004) have shown that the high-strength concrete composite beams had higher initial stiffness and very distinct post-yielding characteristics compared with the normal-strength concrete composite beam. In the composite beams test of studies Nie *et al*.(2004), the concrete compressive strength was up to 84.5 MPa, and the steel beam yield strength was only around 300.0 MPa. Uy B Uy and Sloane(1998) tested composite beams using high strength steel I-section beams with the yield stress up to 690.0 MPa. Besides, extensive experimental studies have been done for the hysteretic behavior of steel composite beams Castro *et al*.(2004), Tagawa *et al*.(1989). So far, few experimental studies focused on the flexural behavior of composite beams with high strength concrete and high strength steel together. Therefore, in this paper, the experiment studies aims to study composite beams with strength of concrete and steel higher than the normal concrete and steel. Composite beams with different engineering material strength and composite beams with same high-strength material but different steel beam depth were tested and investigated. Modes of failure, ultimate load capacity, stiffness and other mechanical behaviors are discussed according to the experiment results.

Table 1 Main experimental parameters

Specimens		SCB1	SCB2	SCB3	SCB6
f_{ys} (MPa)		340.7	450.0	450.0	450.0
f_{us} (MPa)		390.0	481.0	481.0	481.0
f_{cu} (MPa)		34.4	35.2	74.9	76.8
f_{yr} (MPa)		338.0	338.0	338.0	338.0
Steel beam /H × W × t1 × t2(mm)		150 × 130 × 10 × 10			200 × 130 × 10 × 10
Studs spacing (mm)	Transversal	70			
	Longitudinal	190 pure bending, 230 shear span	125 in pure bending span, 200 in shear span		100 pure bending, 150 shear span
Longitudinal reinforcements ratio		1.04%	1.04%	1.04%	1.04%
Transversal reinforcements ratio		1.73%	2.45%	2.45%	2.85%

Notation: f_{ys} = steel yield strength of steel sheet; f_{us} = steel ultimate strength; f_{cu} = concrete strength; f_{yr} = steel yield strength of steel reinforcements; H = height of steel beam; W = width of the top and bottom flanges of steel beam; t1 = thickness of flanges; t2 = thickness of web

2. Experimental program

2.1 Test specimens

A total of four simply-supported composite beams have been constructed and tested. The main experimental parameters are the strength of steel, concrete and steel beam depth, as shown in Table 1. Specimens SCB-1, SCB-2, and SCB3 with the same geometry size are constructed by Q345 steel and C30 normal concrete, Q450 high strength steel and C30 normal concrete, and Q450 high strength steel and C80 high strength concrete, respectively. Specimens SCB-3 and SCB-6, both are constructed with Q450 high strength steel and C80 high strength concrete, whereas with different steel beam depths, 150 mm and 200 mm. Different transversal reinforcement ratios are used for SCB-1, SCB-2, SCB-3 and SCB-6 due to different bending capacities of four beams. Transversal reinforcement ratios for high strength composite beams are improved to avoid the split of concrete slabs before flexural failure.

The detailed geometry of the test beams can be seen in Fig. 1. The concrete slab and the steel beam are directly connected by means of studs. Each of the beams was 4,300 mm long, simply supported on a span of 4,000 mm. By using the depth/span length ratio of about 1/13.3–1/16 for all the beams, the span length of the specimen beams was large enough to minimize the effect of vertical shear and thus to assure a flexural failure.

The section sizes of steel beams satisfy the requirements on slenderness of the flanges and the web of the steel beams for the compact section criteria specified in Eurocode 4 Johnson and Anderson(1993). Shear connections for all the specimens are 1.0, namely full connection. All the specimens are designed in accordance with the simple plastic method.

2.2 Fabrication and construction of test beams

The steel I beams were fabricated from quenched and tempered high strength structural steel. The steel plates were cut, tack welded, and then longitudinal fillets of the beam webs and flanges were reprocessed. Vertical rib stiffeners were tack welded between the top and bottom flanges at support and loading points to minimize distortion and bowing of the steel beams. Stud shear connectors in two

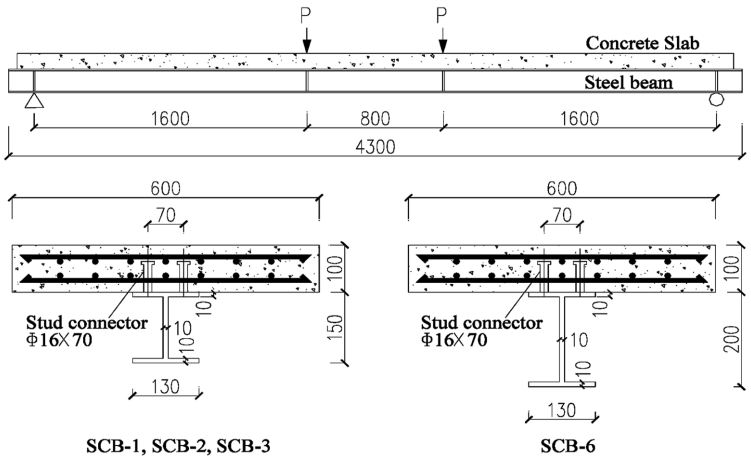

Fig. 1 Test specimens (Units: mm)

longitudinal rows were welded to the top flange with the spacing and quantity required by full shear connection and specifications in Chinese code. The reinforced concrete slab consisted of eight steel bars of diameter 6 mm, in bottom and top layers respectively, along the longitudinal direction. The arrangement of steel bars along the transverse direction varied from different steel beams. For high-strength and high-depth steel beams, high transversal reinforcements ratio was needed to resist the longitudinal splitting in the concrete slabs. Plywood forms were set on the steel beam to allow the concrete slab to be cast. The concrete was poured and vibration was then undertaken with a poker vibrator. The slab was cured under wet hessian until tests took place.

2.3 Material properties

A set of three 150 × 150 × 150 mm^3 concrete cubes were tested to obtain the compressive strength for each composite beam. The compressive strength tests were conducted at two days before each composite beam was tested. The concrete compressive strengths for SCB-1, SCB-2, SCB-3 and SCB-6 were 34.4, 35.2, 74.9, 76.8 MPa respectively at the cure age of 63, 67, 70, and 73 days respectively.

The material properties of all steel and reinforcements were determined by tensile coupon tests. The yield strengths, ultimate strengths, and maximum strain of steel beams were the averages of three coupons from the steel plates. The specimen beams were manufactured from the same batch of steel plates. Hence, the same material properties were used for all the steel beams. The mean tensile yield stress was determined as 340.7 and 450.0 MPa for Q345-steel and Q450-steel coupons respectively, and the mean ultimate stress as 390.0 and 481.0 MPa respectively. The yield strength of steel bars was 338.0 MPa, and the ultimate strength of the studs was 480.0MPa.

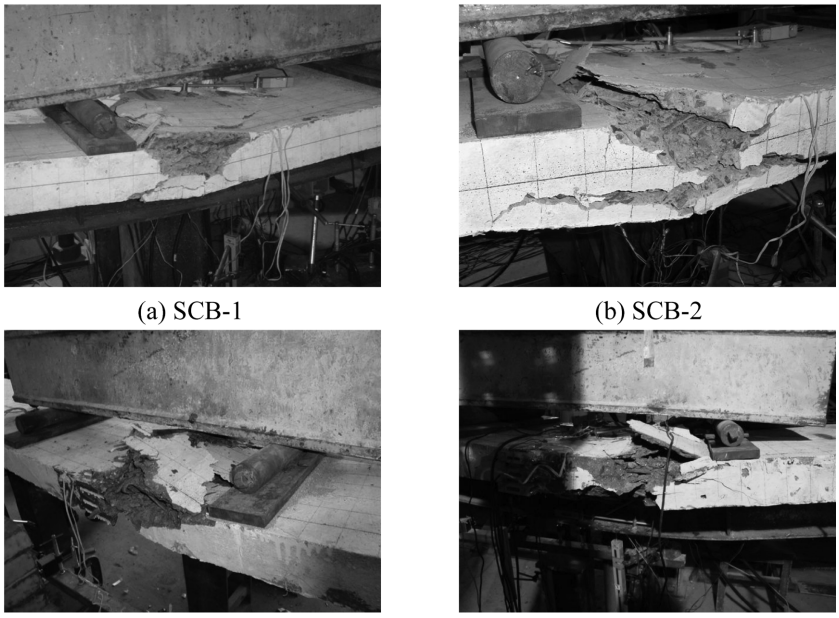

(a) SCB-1 (b) SCB-2

(c) SCB-3 (d) SCB-6

Fig. 2 Failures of composite beams

3. Results and discussions

3.1 General situation

Fig. 2 shows the phenomenon of four steel-concrete composite beams SCB-1, SCB-2, SCB-3 and SCB-6 at failure. It could be observed that the four composite steel-concrete beam specimens exhibited typical flexural failure modes, incurred by the crushing of concrete slabs in the pure bending portion. The failure of SCB-3 and SCB-6 composite beams with Q450-steel and C30-concrete was more brutal and fragile than SCB-1 and SCB-2 composite beams with normal strength concrete. The flexural cracks are more and more massive and extensive from SCB-1 to SCB-3, meanwhile, the buckling of longitudinal bars were more and more severe. In the case of the composite beam SCB-3, the crack spread throughout the pure bending span. For the beam SCB-1, the interface slip between the steel beam and the concrete slab was noticeable. However, no apparent interface slip was observed for composite beams SCB-2, SCB-3 and SCB-6 composite beams.

3.2 Moment and deflection

The curves presented in Fig. 3 show the evolution of the maximum deflection, measured on the bottom of the steel girder at mid-span with the increase of the applied bending moment. It can be seen that, the curves for all the specimens exhibited three stages, the initial elastic behavior, and then transiting into elastic-plastic nonlinear response until reaching the ultimate moment capacity, followed by a descending branch characterizing softening behavior.

For SCB-1, SCB-2, and SCB-3 composite beams with the same geometry but different material strengths, the moment-deflection curves show almost the same elastic-linear response in the early elastic stage. However, significant differences in the response are observed after this initial phase. The response of SCB-1 beam transitioned into nonlinear behaviour at a load of about 80% of its ultimate capacity, accompanied by yielding of the steel beam. Then the load carrying capacity decreased and the post-peak slope is observed to be gentle and smooth, so the mechanical behaviour of SCB-1 beam was relatively ductile. Compared with SCB-1, the transition to nonlinear behaviour of beam SCB-2 occurs

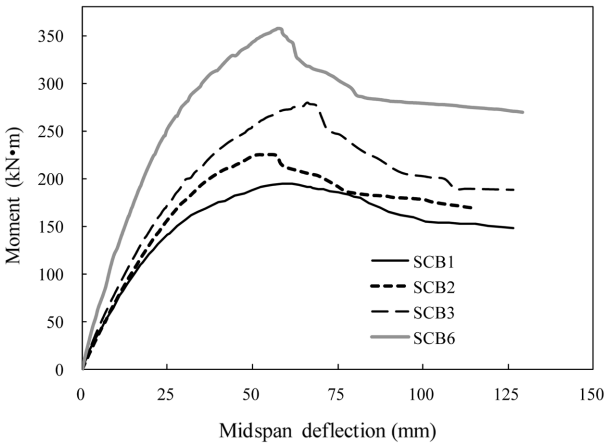

Fig. 3 Moment-deflection curves

later due to its higher steel strength than that of SCB-1. Meanwhile, SCB-2 also attains a much larger load-carrying capacity prior to a sudden load drop. The longest elastic-linear stage is shown in SCB-3 beam. Compared with SCB-2, the moment capacity of SCB-3 beam is significantly higher. This increase is due to the fact that the neutral axis of the SCB-3 beam section is close to the interface between concrete slab and steel beam, so that the large strength potential of both Q450-steel in tension and C80-concrete in compression are fully utilized. On the other hand, the more drastic softening response occurred in the post-peak stage for specimen SCB-3. It should be noted that despite a more brittle failure mode, the deflections at ultimate state for the SCB-3 composite beams are larger than that of specimen SCB-2. Since high-strength concrete is used for SCB-3, the degradation of rigidity is postponed and resistance of concrete slab is effectively enhanced.

In the case of beam SCB-6, the rigidity and moment capacity increase by 26.5% and 55.4% respectively compared to SCB-2 and SCB-3. The deformation abilities for beam SCB-2 and SCB-3 were relatively weak. This can be explained by the fact that, in comparison to SCB-6, the compressive capacity of the concrete slab in SCB-2 is relatively weaker and the heights of both specimens are smaller.

3.3 Moment and curvature

The variations of curvature with bending moment for all the composite beams are shown in Fig. 4. The flexural stiffness *EI* is the slope of the moment-curvature curve.

It can be seen that the flexural stiffness at initial elastic stage, when the moment no more than 100.0kNm, for SCB-1, SCB-2 and SCB-3 are almost the same. However, in the case of SCB-1 beam, stiffness degrades at the load level of 48.7% utmost capacity and then degrades again at the load level of 88.2% utmost capacity. It is a tri-linear curve. Compared to SCB-1, the moment-curvatures of SCB-2 and SCB-3 are bi-linear curve and the variation of their stiffness is similar, although the curvature at failure of SCB-3 is much larger than that of SCB-2. In the case of SCB-6 beam, the flexural stiffness has been improved considerably due to increase of steel beam height. Despite of the divergence of stiffness, the ability of flexural deformation has few discrepancies, curvature at failure of SCB-6 approached to that of SCB3.

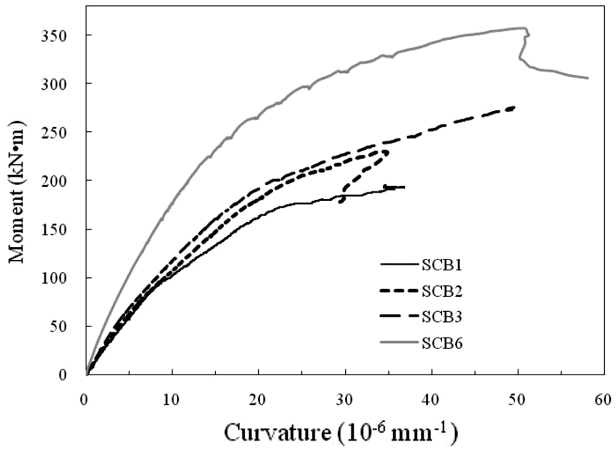

Fig. 4 Moment-curvature curves

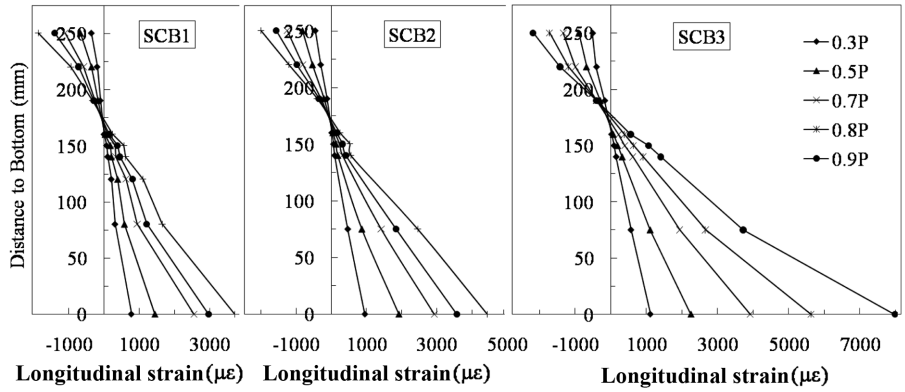

Fig. 5 Longitudinal train distributions at the mid-span section

3.4 Strain

Fig. 5 presents longitudinal strain distributions at the mid-span section for specimen SCB-1, SCB-2 and SCB-3. It should be noted herein that longitudinal strain results for SCB-6 is not shown in the Figs. 5-7 due to its different height from the other three specimens and little comparison value. P shown in the figure was the maximum load capacity. It can be seen that the neutral axis in the section shifts slightly although it always exists in the concrete slab and very close to the interface of steel and concrete. As for SCB-1 and SCB-2 composite beams, noticeable strain gaps (slip strain) between the strains of concrete flange soffit and steel top flange occur due to the influence of slips along the interfaces of steel beams and concrete slabs in shear spans, when the load reached 90% of maximum capacity. However there is no apparent slip strain during the whole loading process in the case of SCB-3 beam. When the load is no more than 70% of maximum capacity, the longitudinal strains distributed in the section are approximately along the linear trend, so the plane cross section assumption can be applied in analysis of composite beams behavior. It can be easily found in Fig. 5 that for SCB-1 beam, the slops of stain distribution lines close to the bottom of steel beam decrease apparently when the loads larger than 70% of maximum capacity. It indicates that steel fibers close to the bottom of steel beam enter the yield stage. SCB-2 beam is quite different. It can be explained by that the strain corresponding to yield stress for SCB-1 beam with Q345-steel is about 30% larger than that of SCB-2 beam with Q450-steel. In the case of SCB-3 beam, due to the improved strength of concrete resulting in the postponing of failure in concrete slab, the strength of steel beam have been made full use of compared to SCB-1 and SCB-2 beams. Shown as Fig. 5, the largest longitudinal strain developed in the steel beam is about 9,000 $\mu\varepsilon$, 80% larger than that of SCB-1 and SCB-2 beams.

Figure 6 shows the distribution of the transversal strain measured on the top surface of the concrete slab for SCB-1, SCB-2 and SCB-3 beams along the length axis of the composite beams. These measured results can indicate the resistance to longitudinal slitting of concrete slabs. It is obvious that all the concrete transversal strains obtained are positive, tensile strain. The measured maximum strains are logically located near the mid-span of composite beams, and the strains decrease gradually towards the beam end. It means that the concrete slabs trend to be split and apparent relatively close to the mid-span. The stain value and distributions of SCB-1 and SCB-2 are almost the same, up to 1,900 $\mu\varepsilon$. However, the stains for SCB-3 beam are no more than 1000 $\mu\varepsilon$. The favorable results show that the improvement strength of concrete can enhance the resistance of slabs to split effectively.

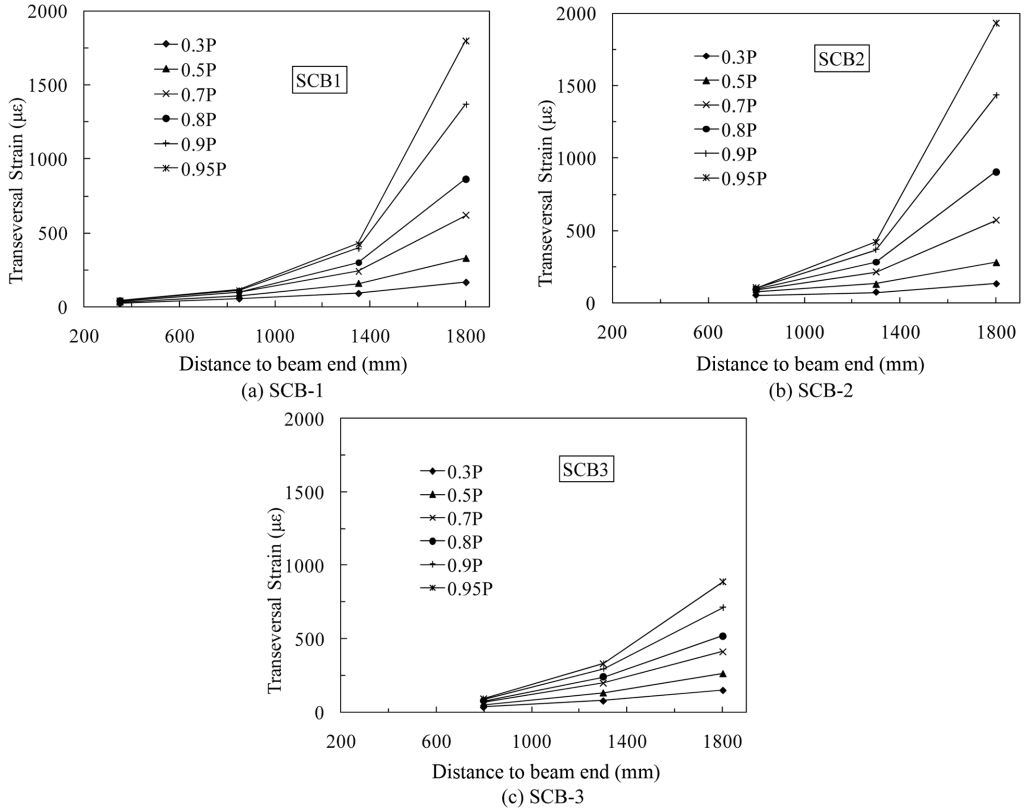

Fig. 6 Transversal concrete train distributions for SCB-1, SCB-2 and SCB-3

3.5 Interface slip

Fig. 7 presents the evolution of the relative slip along the interface of the concrete flange and the steel beam with the increase of the applied load for the beams SCB-1, SCB-2 and SCB-3. The linear potentiometers to detect slips were set at a spacing of 500 mm, one eighth of the clear span, along half span of the composite beams. It can be easily found that the slip increased drastically from the mid-span towards to one fourth of span. As for SCB-1 beam, the measured maximum interface slip is up to 0.7 mm, occurring at 1,000 mm to the beam end, shown as Fig. 7(a). As for SCB-2 beam, the slip develops due to the increasing of distance to mid-span. The measured maximum interface slip is 0.52 mm, located at the beam end, shown as Fig. 7(b). Compared to SCB-1 and SCB-2 beams, unconspicuous interface slips take place in SCB-3 beam, with the maximum slip value of 0.3mm when the beam near to be failure, shown as Fig. 7(c).

3.6 Comparisons with code results

Design codes China Academy of Building Research(2003), Johnson and Anderson(1993) offer the methods to calculate the strength of steel-concrete composite beams. In this paper, the moment capacities of the four specimens calculated according to Eurocode 4 Johnson and Anderson(1993) are compared

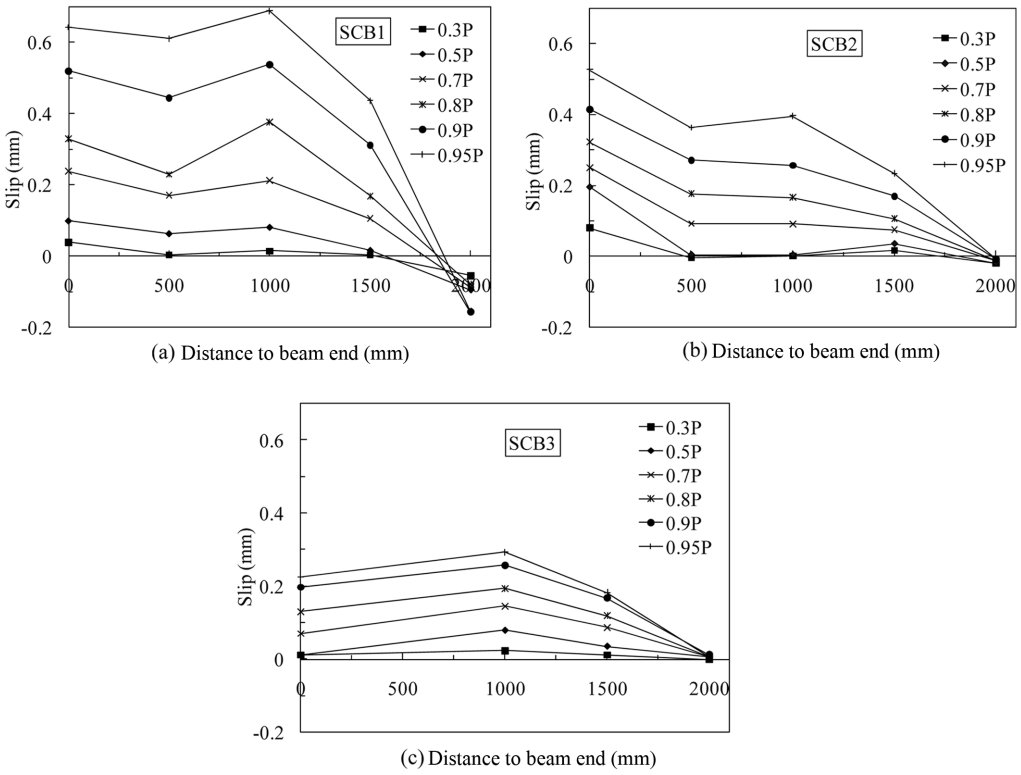

Fig. 7 Interface slip along the beam length

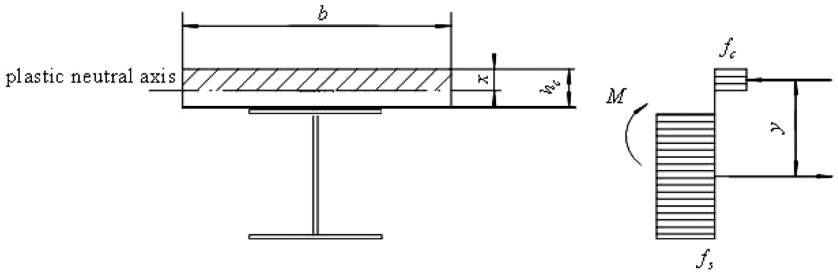

Fig. 8 Stress distributions for a composite beam in bending

with the experiments results so as to explore the applicability of the codes to guide the design of high-strength composite beams. It should be noted that the concrete strength used in calculation is cylinder concrete strength required in Eurocode 4, which is converted from cube strength according to Mansur and Islam(2002).

Shown as Fig. 8, the plastic neutral axis position can be obtained by comparing the tensile plastic force of steel F_s and the compressive force of concrete F_c. For all the tested composite beams SCB-1, SCB-2, SCB-3 and SCB-4, the plastic neutral axis is located in the concrete slab.

Table 2 Comparison between code and experimental results

	SCB1	SCB2	SCB3	SCB6
Material strength	C30-concrete Q345-steel	C30-concrete Q450-steel	C80-concrete Q450-steel	C80-concrete Q450-steel
M_c / kNm	183.8	222.1	268.4	348.1
M_t / kNm	195.1	230.2	282.7	357.7
M_c / M_t	0.942	0.965	0.949	0.973

Therefore, the calculated moment capacity can be obtained by the following equations:

$$M = bxf_c y \tag{1}$$

$$x = Af_y/(bf_c) \tag{2}$$

with M = bending moment capacity, b = width of the concrete slab, x = depth of the compression region of the concrete slab, A = cross-sectional area of the steel beam section, y = distance between the cancroids of the steel beam section and the center of compression region in the concrete slab, f_c = the compressive strength of concrete, and f_s = the tensile strength of steel.

Table 2 presents the calculated moment capacities and the corresponding test results. The moment capacities from experiments in this paper are slightly larger than the corresponding results of ultimate strength from "Eurocode 4: Design of Composite Steel and Concrete Structures" shown as Table 2. There are a few more reasons which may have attributed to the inaccuracies which include the inability of most the steel tension fibers have not reached yield when the concrete collapsed. Due to the less ductility of high strength materials, the actual stress distribution at the failure, in which the steel tension fibers were unable to be fully strain hardened, is quite different from stress block distribution, which is assumed in the codes is applicable for composite beams with normal-strength material but not for those with high strength material.

4. Conclusions

This paper has briefly presented the experimental studies on composite beams constructed with different strength steel beam and different strength concrete slab. The effects of high-strength steel and concrete on the mechanical behavior of composite beams have been explored. The following conclusions can be drawn from the research.

The failure of composite beams with high-strength steel or/and concrete is brittle, compared to beams with normal-strength steel and concrete. However, the former has quite improved moment capacity. The high-strength concrete slab has stronger resistance to the longitudinal split than normal-strength concrete slab. Furthermore, no apparent slip occurred in the high-strength composite beams. The flexural strength based on current codes may be not conservative slightly for predicating the moment capacity of composite beams with high-strength steel or concrete. Further experiment and simulation investigations need to be conducted to propose the more accruable calculation methods for high-strength composite beams.

Acknowledgements

The authors appreciate the financial support provided by the project from the National Natural Science Foundation of China (Grant No. 50838004) gratefully.

References

Amadio, C., Fedrigo, C. and Fragiacomo, M. (2004), "Experimental evaluation of effective width in steel-concrete composite beams", *J. Construct. Steel Res*., **60**(2), 199-220.

American Institute of Steel Construction (1994), Load and resistance factor design specification for structural steel buildings, *Eng. J-AISC*, Chicago.

Architectural Institute of Japan (1987), *AIJ: Standards for structural calculation of steel reinforced concrete structures*, AIJ, Tokyo, Japan.

Bullo, S. and Di Marco, R. (2004), "A simplified method for assessing the ductile behavior of stud connectors in composite beams with high strength concrete slab", *J. Constr. Steel. Res.*, **60**(9), 1387-1408.

Castro, J.M., Elghazouli, A.Y. and Izzuddin, B.A. (2004), "Modeling of the panel zone in steel and composite moment frames", *Eng. Struct.*, **27**(1), 129-144.

China Academy of Building Research (2003), Code for design of steel structures(GB 50017-2003), China Architecture and Building Press, Beijing.

El-Tawil, S. and Deierlein, G.G. (2001), "Nonlinear analyses of mixed steel-concrete moment frames", *J. Struct. Eng-ASCE*., **127**(6), 647-655.

Johnson, R.P. and Anderson, D. (1993), *Designers' guide to EN1994-1-1: Eurocode4: design of composite steel and concrete structures*, *Part1-1: general rules and rules for building*, CEN, Brussels.

Lam, D. and EI-Lobody, E. (2005), "Behavior of headed stud shear connectors in composite beam", *J. Struct. Eng-ASCE*., **131**(1), 96-107.

Liew, J. Y. R., Chen, H. and Shanmugam, N.E. (2001), "Inelastic analysis of steel frames with composite beams" *J. Struct. Eng-ASCE.*, **127**(2), 194-202.

Mansur, M. and Islam, M.M. (2002), "Interpretation of concrete strength for nonstandard specimens", *J. Mater. Civil. Eng.*, **14**(2), 151-155.

Nie, J.G., Xiao, Y. and Tan, Y. (2004), "Experimental studies on behavior of composite steel high-strength concrete beams", *ACI Struct. J.*, **101**(2), 245-251.

Nie, J.G., Qin, K. and Cai, C.S. (2008), "Seismic behavior of connections composed of CFSSTCs and steel-concrete composite beams-experimental study", *J. Constr. Steel. Res.*, **64**(10), 1178-1191.

Richard Liew, J.Y. (2001), "State-of-the-art of advanced inelastic analysis of steel and composite structures", *Steel. Compo. Struct.*, **1**(3), 341-354.

Salari, M. R. and Spacone, E. (2001), "Analysis of steel-concrete composite frames with bond-slip" *J. Struct. Eng*., **127**(11), 1243-1250.

Spacone, E. and EI-Tawil, S. (2004), "Nonlinear analysis of steel-concrete composite structures: state of the art", *J. Struct. Eng-ASCE*., **130**(2), 159-168.

Tagawa, Y., Kato, B. and Aoki, H. (1989), "Behavior of composite beams in steel frame under hysteretic loading", *J. Struct. Eng-ASCE.,* **115**(8), 2029-2045.

Uy, B. and Sloane, R.J. (1998), "Behavior of Composite Tee Beams Constructed with High Strength Steel", *J. Constr. Steel. Res.*, **46**(1-3), 203-204.

Viest, I.M., Colaco, J.P., Furlong, R.W. and Griffes, L.G. (1997), *Composite construction: design for buildings*, McGraw-Hill, New York.

Xue, W. and Yang, F. (2009), "Experiment research on seismic performance of prestressed steel reinforced high performance concrete beams", *Steel. Compos. Struct.*, **9**(2), 159-172.

Yuan, Y., Zhao, H.L. and Bao, X.F. (2008), "Design for a large underground space", *Proceedings of the Institution of Civil Engineers-Municipal Engineer*, Issue MEI, 35-41.